Annals of Work Exposures and Health, 2020, Vol. 64, No. 1, 38–54
doi: 10.1093/annweh/wxz088
Advance Access publication 10 December 2019
Original Article

Original Article

Workplace Emissions and Exposures During Semiconductor Nanowire Production, Post-production, and Maintenance Work

Christina Isaxon[1,2,*], Karin Lovén[1,2], Linus Ludvigsson[1,3], Sudhakar Sivakumar[1,3], Anders Gudmundsson[1,2], Maria E. Messing[1,3], Joakim Pagels[1,2], and Maria Hedmer[1,4]

[1]NanoLund, Lund University, Box 118, SE-22100 Lund, Sweden [2]Ergonomics and Aerosol Technology, Lund University, SE-22100 Lund, Sweden [3]Solid State Physics, Lund University, SE-22100 Lund, Sweden [4]Occupational and Environmental Medicine, Lund University, SE-22100 Lund, Sweden

*Author to whom correspondence should be addressed. e-mail: christina.isaxon@design.lth.se

Submitted 19 October 2018; revised 6 September 2019; editorial decision 12 October 2019; revised version accepted 6 September 2019.

Abstract

Background: Nanowires are a high-aspect-ratio material of increasing interest for a wide range of applications. A new and promising method to produce nanowires is by aerotaxy, where the wires are grown in a continuous stream of gas. The aerotaxy method can grow nanowires much faster than by more conventional methods. Nanowires have important properties in common with asbestos fibers, which indicate that there can be potential health effects if exposure occurs. No conclusive exposure (or emission) data from aerotaxy-production of nanowires has so far been published.
Methods: Different work tasks during semiconductor nanowire production, post-production, and maintenance were studied. A combination of direct-reading instruments for number concentration (0.007–20 μm) and filter sampling was used to assess the emissions (a couple of centimeter from the emission sources), the exposure in the personal breathing zone (max 30 cm from nose–mouth), and the concentrations in the background zone (at least 3 m from any emission source). The filters were analyzed for metal dust composition and number concentration of nanowires. Various surfaces were sampled for nanowire contamination.
Results: The particle concentrations in the emission zone (measured with direct-reading instruments) were elevated during cleaning of arc discharge, manual reactor cleaning, exchange of nanowire outflow filters, and sonication of substrates with nanowires. In the case of cleaning of the arc discharge and manual reactor cleaning, the emissions affected the concentrations in the personal breathing zone and were high enough to also affect the concentrations in the background. Filter analysis with electron microscopy could confirm the presence of nanowires in some of the air samples.
Conclusions: Our results show that a major part of the potential for exposure occurs not during the actual manufacturing, but during the cleaning and maintenance procedures. The exposures and

emissions were evaluated pre- and post-upscaling the production and showed that some work tasks (e.g. exchange of nanowire outflow filters and sonication of substrates with nanowires) increased the emissions post-upscaling.

Keywords: direct-reading instruments; electron microscopy; metal analysis; occupational exposure; upscaling

Introduction

Nanomaterials generally refer to engineered structures, where industry utilizes the fact that particles smaller than about 100 nm exhibit remarkable properties—e.g. physical, chemical, and electronic—that are different from the properties of the corresponding bulk material. The European Union has recommended the following definition of nanomaterial: 'Nanomaterial' means a natural, incidental, or manufactured material containing particles, in an unbound state or as an aggregate or as an agglomerate and where, for 50% or more of the particles in the number size distribution, one or more external dimensions are in the size range 1–100 nm (European Commission, 2011). Reporting requirements with this criterion as key element of nanomaterial identification are now legally required in several EU countries, e.g. Denmark, Belgium, and Germany (Contado, 2015). The diversity of nanoparticles, and products which incorporate nanomaterials, are increasing on a daily basis, and nanotechnology is often referred to as one of the most exciting industrial innovations of the 21st century.

The production of and demand for engineered high-aspect-ratio nanomaterials is growing, with carbon nanotubes being one of the most common of these fiber-shaped materials. WHO defines fiber materials as insoluble fibers having a length >5 µm, a width <3 µm, and a length-to-diameter ratio >3 (WHO, 1986, 1997). Carbon nanotubes are used in several industrial applications, for example, incorporated into materials such as plastics, rubbers, composites, textiles, and concrete to improve the characteristics of the material (Barkauskas et al., 2010; McIntyre, 2012). Nanowires are another form of fiber material that is one-dimensional (1D) rod shaped (Kane et al., 2018) and differ from carbon nanotubes mainly in that they are not hollow structures. Nanowires have a diameter in the size range of tens of nanometers and a typical length of a few micrometers. Nanowires can be built up from a variety of materials such as metals, metal chalcogenides, metal carbides, oxides, and semiconductors (Messing et al., 2009). Semiconductor nanowires are normally made of III–V materials (a combination of materials from groups III and V in the periodic system), these can, for example, be gallium arsenide (GaAs), GaP, InP, and GaSb. Nanowires do not have the tensile strength of carbon nanotubes and are used for other types of applications, such as for the next generation of light emitting diodes (Qian et al., 2005), batteries (Chan et al., 2008), and solar cells (Wallentin et al., 2013). Being key building blocks for these types of new emerging technologies, the commercial interest in nanowires is increasing and is likely to continue doing so (Poland, 2011). Nanowires are commonly grown by epitaxy, where growth in one dimension is enhanced by metal seed particles on a single-crystalline substrate (Yazawa et al., 1992). The nanowire structures are grown under the seed particles by using, e.g. metalorganic vapor-phase epitaxy, molecular-beam epitaxy, or chemical-beam epitaxy. These methods are, however, slow and costly (Heurlin et al., 2012). A new, upcoming method for synthesizing nanowires directly in gas-phase has been developed, *Aerotaxy*, which is expected to have substantial impact on how the field of nanoscale devices will develop in the future (Heurlin et al., 2012). In aerotaxy, size-selected particles are used as seed particles, these are mixed with gas-phase reactants, and heated for a well-controlled period. After wires have formed in the continuous stream of gas they are transported—still in aerosol phase—to a chamber where they are deposited by an electric field onto a substrate. Currently, GaAs nanowires are grown using gold seed particles, and trimethylgallium and arsine as precursor gases, but the method is general and other common precursor materials and techniques of seed particle formation can be used. GaAs as compound is a widely used in semiconductor applications in the microelectronics industry (Tanaka, 2004).

If inhaled, the fiber shape is a well-known reason for concern. The reduced aerodynamic diameter of the particle enables deposition beyond the ciliated airways despite its length (the particle aligns with the airflow). Once deposited in the alveoli, the fiber is too long (>5 µm) to be completely engulfed by macrophages, resulting in frustrated phagocytosis and in that the particle cannot be effectively cleared from the alveoli, resulting in an accumulation over time and lung disease (Donaldson et al., 2010). According to a recent review about the asbestos-carbon nanotubes analogy, the fiber pathogenicity paradigm has been extended to include also nanowires (Kane et al., 2018).The aim of this study was to characterize exposure and emissions of aerotaxy produced

semiconductor nanowires and to evaluate how process upscaling can affect exposure. Measurements were conducted during production, post-production, and maintenance of the production equipment. The potential for secondary inhalation exposure, caused by resuspension of particles deposited on various surfaces, and dermal exposure from these surfaces was also assessed.

Methods

Facilities

An intervention study was conducted where measurements were performed twice (in 2014 and 2016), hereafter "Study 1" and "Study 2", at a producer of GaAs nanowires by the aerotaxy method. The GaAs nanowires are grown while gas borne using catalytic seed aerosol nanoparticles of gold size selected by a differential mobility analyzer (DMA) by addition of gaseous precursor molecules of arsine and trimethylgallium in closed reactor systems (Heurlin et al., 2012). Study 1 was conducted pre-upscaling the production and Study 2 post-upscaling (larger facility and larger quantities). After Study 1, the nanowire producer received feedback through a measurement report and took the information into consideration in the construction of a new larger reactor. A least one work task (manual reactor cleaning) was therefore no longer performed during Study 2. The primary produced nanowires had a target production length of 1 µm and diameter of 120 nm. The upscaling amounts to an increase in produced material mass of approximately three orders of magnitude. The same or similar processes were studied during both measuring periods to be able to evaluate possible improvements that had been implemented, as well as the effects of upscaling the processes.

GaAs nanowires were synthesized in the production laboratory, located at one address during Study 1 but at another address during Study 2. The work involving handling of silicon (Si) nanowires (used as example nanowires for exposure evaluations) on substrates and in liquid took place in the post-production laboratories. These laboratory rooms were located at the Study 2 address, both during Studies 1 and 2. However, the specific work tasks were performed in different laboratory rooms during the different studies.

Work tasks

A number of different work tasks were performed during the two studies. Table 1 shows these different work tasks and a more detailed description of what they entailed, as well as during which Study (1/2) they were conducted and measured. Inspection of reactor, and automatic reactor cleaning, was still performed during Study 2, but due to the scheduling at the producer, it was not possible to measure these work tasks at that time. After upscaling, the arc discharge was cleaned every day, and the DMA was cleaned every other week.

Engineering controls

During the different work tasks, different types of exposure control techniques and enclosures were used. These included a ventilated cupboard, open during some work tasks, laminar air flow (LAF) bench, glove box, and a completely closed reactor system. Some work tasks were performed without any engineering controls, on an open bench. Table 1 shows the specific details for which type of engineering controls that were present at which work task.

Personal protective equipment (PPE)

The different PPEs used during the different work tasks included respiratory protection and different protective clothing. A full face mask with both gas filter (ABE) and particle filter (P3) was used for respiratory protection. Cleanroom gowns were used together with gloves made of nitrile, shoe covers, and hairnet during some of the work tasks in the production laboratory, while disposable coveralls, shoe protection, and gloves made of nitrile were used for other work tasks. In the post-production laboratory, a protective gown and gloves made of nitrile were used. Table 1 shows the specific details for which type of protection that was used during which work task.

Sampling strategy

Both on-line and filter-based methods were used to carry out particle measurements in four different measuring zones. The *emission zone* was defined as the zone closest to the potential particle source, typically no more than a few centimeters. The *personal breathing zone* was defined as a radius of 30 cm around the nose and mouth of the worker carrying out the work process. The *background zone* was defined as at least 2–3 m from any potential particle source. The *supply air* (general ventilation) was also measured. The on-line, or direct reading, instruments were used to evaluate which specific processes gave rise to potential particle exposures, while the filter measurements were used to confirm the specific type of exposure and the average concentrations.

Air sampling methods and analyses

Filter sampling for total dust and metal composition analysis

Time-integrated emission zone, personal breathing zone, and background zone samples of total dust were collected on 25-mm cellulose fiber filters with a pore size

Table 1. Work tasks performed at the nanowire (NW) producer, when the processes were evaluated, which engineering controls that were present and which type of personal protective equipment (PPE) that were used by the workers.

Work task	Work task description	Study 1/2	Engineering controls	PPE
		Production laboratory		
Cleaning of seed aerosol particle generator (*Study 1*: high temperature furnace *Study 2*: arc discharge)	*Study 1*: The lid and bottom of the furnace were removed and cleaned with a brush and a drill. The tubing was cleaned with compressed air. *Study 2*: The arc was disassembled and the different parts were cleaned with a brush.	1/2	Open ventilated cupboard/Open bench	Full face mask (ABE+P3), cleanroom gown, gloves, shoe covers, hairnet
Cleaning of DMA and aerosol filter exchange	The DMA was disassembled and cleaned with a brush and ethanol. Some parts were cleaned with compressed air. The aerosol filter was changed.	1/2	Open ventilated cupboard/open LAF bench	Full face mask (ABE+P3), cleanroom gown, gloves, shoe covers, hairnet
Inspection of reactor	The top of the reactor was opened and the inside was inspected with an endoscope.	1	Ventilated cupboard	Full face mask (ABE+P3), disposal coveralls, shoe protection, gloves
Automatic reactor cleaning	Computer work was performed. The reactor was automatically cleaned with nitrogen gas.	1	Ventilated cupboard	Full face mask (ABE+P3), disposal coveralls, shoe protection, gloves
Manual reactor cleaning	The reactor was opened and manually cleaned with a steel wire and a cleanroom vacuum cleaner.	1	Ventilated cupboard	Full face mask (ABE+P3), disposal coveralls, shoe protection, gloves
Exchange of NW outflow filter(s)	Tubes were disconnected, holders were cleaned with ethanol, and filter(s) were exchanged.	1/2	Open ventilated cupboard	Full face mask (ABE+P3), cleanroom gown, gloves, shoe covers, hairnet
Leak test	Different parts of the reactor cupboard were opened, leak tests were performed with helium.	2	Open ventilated cupboard	Full face mask (ABE+P3), cleanroom gown, gloves, shoe covers, hairnet
Work in glove box	GaAs NWs were being harvested.	1/2	Glove box with over-pressure	Cleanroom gown, gloves, shoe covers, hairnet
Production of GaAs NWs	Computer work was performed. Supervision of the production was conducted.	1/2	Closed system	Cleanroom gown, gloves, shoe covers, hairnet
		Post-production laboratory		
Sonication of substrates with Si NWs	Substrates with Si NWs (grown from gold seed particles) were transferred into liquid and sonicated. Work bench was cleaned.	1/2	LAF bench/Open bench	Eye googles, protective gown, gloves/Full face mask (ABE+P3), protective gown, gloves
Handling of substrates with Si NWs	Substrates with Si NWs (grown from gold seed particles) were shaken in an open box and transferred to another box.	2	Parts in LAF bench, parts on open bench	Full face mask (ABE+P3), protective gown, gloves

of 0.45 µm (SKC Inc., USA) mounted in three-piece filter cassettes made of conductive polypropylene. An Escort ELF pump (MSA, USA) was used to provide the sample flow (open-face sampling). The air flow rate was before, during, and after the sampling regularly checked with a primary calibrator (TSI model 4100, TSI Inc., USA). The filter samples were analyzed gravimetrically for total dust according to a validated method at University and Regional Laboratories, Region Skåne, Sweden. The filters were pre- and postweighed using an analytical balance (XP105 DeltaRange Excellence Plus, Mettler Toledo, Switzerland). The limit of detection (LOD) of the gravimetric method was determined to 0.05 mg/sample. The difference between post- and preweight was corrected with the mean value of field blank filter weight change.

The metal composition of the total dust filter samples was quantified. The filter samples were worked up by digestion with 1 ml conc. nitric acid (nitric acid, trace metal grade, Fisher Chemicals) in an oven (60°C) for 16 h, and then diluted to 10 ml with Milli-Q water to a stock solution. Analysis was performed by inductively coupled plasma-mass spectrometry (ICP-MS, iCAP Q, Thermo Scientific, Bremen, Germany), and elements such as Ga and As were detected. The LOD for each element was calculated as three times the standard deviation of blank filters. The LOD was 0.25 ng/sample for Ga and 0.50 ng/sample for As. All results were blank filter corrected.

Filter sampling for SEM analysis

Time-integrated emission zone, personal breathing zone, and background zone samples were collected by open-face sampling on 25-mm polycarbonate filters with a pore size of 0.4 µm (SKC Inc.) mounted in filter cassettes. A sampling pump (MSA) sucked air through the filter. The air flow was before and after the sampling checked with a primary calibrator (TSI Inc.). The filter samples were analyzed by scanning electron microscopy (SEM) analysis, including energy dispersive X-ray spectroscopy (EDX). A number of areas (15–20) per filter were randomly chosen for image acquisition. As SEM does not reveal whether or not particles in clusters are stuck solid to each other or loosely piled up, clusters are treated as one particle and measured as one. The uncertainty of attributing dimensions to subparts of clusters would be too high, as parts of the cluster are covering other parts. In 2014, the fiber LOD was determined to be between 0.025 and 3.1/cm^3 NWs (depending on sampling time) for filter samples.

Direct reading instruments

Several different direct-reading instruments (summarized in Table 2) were used for time resolved studies of the particle emissions. The particle number concentration and the aerodynamic diameter of particles with a size between 0.5 and 20 µm were measured with two Aerodynamic Particle Sizers (APS, model 3321, TSI Inc.) with a time resolution of 5 s. A condensation particle counter (CPC, model 3775, TSI Inc.) measured the total number concentration of particles >0.007 µm, with a time resolution of 1 s. A scanning mobility particle sizer (SMPS: DMA 3071, TSI Inc. and CPC 3010, TSI Inc.) measured the number concentration and the mobility size distribution of particles between 0.01 and 0.5 µm, with a time resolution of 2.5 min. One APS and the CPC measured in the emission zone, while the second APS and the SMPS (only the CPC 3010 during Study 2, with a time resolution of 1 s) were measuring in the background zone.

Additionally, a Nanotracer (NT, Philips Aerasense, the Netherlands) was carried by the worker in order to measure the number concentration of particles smaller than 0.3 µm (time resolution 16 s) in the personal breathing zone. During Study 2, a second Nanotracer was carried by a worker not directly involved in the work tasks but residing in the production laboratory. To further evaluate the personal breathing zone during Study 2, the worker was also carrying a SidePak (model AM510, TSI Inc.) for mass concentration of particles 0.1–10 µm, with a time resolution of 1 s.

For particle measurements in the room ventilation air, a P-Trak (model 8525, TSI Inc.) and a DustTrak (model DRX 8534, TSI Inc.) were used to assess the particle number concentration and the particle mass concentration, respectively, with a time resolution of 1 s.

The direct reading instruments were run side-by-side over the lunch breaks during all study days, to confirm

Table 2. Direct reading instruments used for the time resolved studies of the particle emissions.

	Personal breathing zone	Emission zone	Background zone	Ventilation
Study 1 (2014)	NT	APS, CPC	APS, SMPS	P-Trak, DustTrak
Study 2 (2016)	NT, SidePak	APS, CPC	APS, CPC, NT	P-Trak, DustTrak

NT, Nanotracer; APS, Aerodynamic Particle Sizer; CPC, Condensation Particle Counter; SMPS, Scanning Mobility Particle Sizer.

that there were no significant differences between the two Nanotracers, between the two CPCs and between the two APS instruments.

Sampling of arsine gas

Time-integrated emission zone and personal breathing zone sampling of arsine gas were conducted during Study 1 by using a solid sorbent tube with charcoal (SKC Inc.) connected to a sampling pump (MSA). A particle filter was placed in front of the solid sorbent tube. The air flow was before and after the sampling checked with a primary calibrator (TSI Inc.). The solid sorbent tubes were eluted with 4 ml 2% nitric acid (nitric acid, trace metal grade, Fisher Chemicals). The elute was then analyzed with ICP-MS (iCap Q, Thermo Scientific, Bremen, and Germany). The results were corrected with solid sorbent tube blanks. The LOD was 3.0 ng/sample for As.

Surface sampling method and analysis

A tape sampling method (Hedmer et al., 2015) was used to collect surface samples. Ordinary transparent adhesive tape (Staples Europe B.V., Amsterdam, the Netherlands) was used with a width of 15 mm and length of 15 cm. Single tape samples were collected from various surface locations. A new pair of nitrile gloves was used for each collected tape sample. One or two field blanks were also collected in each laboratory. SEM/EDX analysis of the tape samples were performed at Solid State Physics, Lund University. In 2014, the LOD was determined to be >0.022 µm in size [one pixel], and >500 #/sample.

The tape sampling method was evaluated for GaAs nanowires by determination of the collection efficiency. Aerotaxy produced GaAs nanowires were deposited on five smooth metal surfaces and the number of nanowires at each surface was determined by SEM analysis. The surfaces were then tape sampled according to the published method and the tape samples were analyzed by SEM to establish the collection efficiency factor, which was determined to be 60–91% (average 72%).

Results

Filter sampling

Table 3 shows results from the filters with load above LOD. Note that some of the filter samples have been sampling for more than one work task (according to Table 1) and that others have been divided into multiple filter samples within one work task. The total dust determination analysis (not included in Table 3) showed one filter just at the LOD from Study 1 (work task: sonication of substrates with Si NWs, specific activity of cleaning the bench) with 0.05 mg/m^3 and one filter during Study 2 (work tasks: cleaning of arc discharge and DMA and aerosol filter exchange) with 0.4 mg/m^3.

Cleaning of arc discharge and DMA and aerosol filter exchange

Fig. 1 shows the total particle number concentration in the production laboratory during Study 2, during cleaning of arc discharge and DMA and aerosol filter exchange. Measurements from the CPCs (>0.007 µm), Nanotracers (0.01–0.3 µm), and the P-Trak (0.02–1 µm) are presented. The SidePak did not show any significant particle increases in the breathing zone. An increase in particle concentration can be seen shortly after the work task began, when the arc discharge was being cleaned. During Study 1, cleaning of the high temperature furnace (which at that time was used for seed particle generation), only showed a short, low particle peak in the APS placed in the emission zone. Cleaning of DMA and aerosol filter exchange did not generate any significant particle emissions during either of the studies.

SEM and EDX analysis of the filters sampled during cleaning of arc discharge and DMA and aerosol filter exchange (Study 2) confirmed the presence of gold nanoparticles and agglomerates both in the emission zone (Fig. 2a) and the personal breathing zone (Fig. 2b).

Manual reactor cleaning

Increased particle number concentrations occurred in the emission zone in Study 1 during manual reactor cleaning (Fig. 3), for particles both in the nanometer range and in the micrometer range. This emission affected the background concentration for the remainder of the work task. About 1 min after the peak in the emission zone, a corresponding particle increase (about 5000 cm^{-3}) could also be detected in the personal breathing zone (not shown here). Fig. 4a shows the aerodynamic particle size distribution from the emission and the background zone during the initial peak in Fig. 3 (at ~10:26). Fig. 4b shows the aerodynamic particle size distribution from the emission and the background zone during the end of the work task (at ~10:34).

Fig. 5 shows parasitically grown GaAs nanowires (uncontrolled and unwanted growth which can occur in the reactor) sampled in the emission zone (Fig. 5a) during manual reactor cleaning and in the personal breathing zone (Fig. 5b) during all the work performed in the production laboratory. The SEM analysis showed

Table 3. Filter results for the work tasks, and filter background results, with results over the LOD. Number concentration of nanowires from SEM analysis and metal dust composition from ICP-MS.

Work task	Sampling time (min)	SEM analysis		Metal dust composition (ng/m^3)	
		Detection of nanomaterial (Yes/No)/type	Number conc. NW (cm^{-3})	Ga	As
Study 1 (2014)					
Personal breathing zone					
All work tasks performed in the production laboratory	247	Yes/GaAs NWs	0.025	30	10
Emission zone					
Cleaning of high temperature furnace	18	No	<LOD	10	ND
Inspection of reactor	6	No	<LOD	40	ND
Automatic reactor cleaning	18	No	<LOD	30	ND
Manual reactor cleaning	10	Yes/GaAs NWs	98	8200	2300
Background zone					
All work tasks performed in the production laboratory	455	No	NS	40	10
Study 2 (2016)					
Personal breathing zone					
All work tasks performed in the production laboratory	256	Yes/gold nanoparticles	<LOD	20	40
All work tasks performed in the production laboratory (worker in the background)	289	No	<LOD	1	ND
Emission zone					
Cleaning of arc discharge and DMA and aerosol filter exchange	107	Yes/gold nanoparticles	<LOD	20	30
Exchange of NW outflow filter	8	No	<LOD	510	3600
Work in glove box and production of GaAs NWs	75	No	<LOD	20	3
Sonication of substrates with Si NWs	96	Yes/Si NWs	*	ND	ND
Background zone					
All work tasks performed in the production laboratory	403	No	<LOD	5	2

ND, not detected; NS, not sampled.
*Not possible to determine.

nanowire number concentrations of 98 cm^{-3} in the emission zone and 0.025 cm^{-3} in the personal breathing zone. The characteristics of the counted nanowires in Study 1 are presented in Table 4.

Exchange of NW outflow filter(s)

Fig. 6 shows the total particle number concentration in the production laboratory in Study 1 (Fig. 6a) and Study 2 (Fig. 6b) during exchange of NW outflow filter(s). During Study 1, three filters were exchanged and minor particle increases can be seen during these activities. During Study 2, only one filter was exchanged, however, a major increase in particle number concentration (note the difference in the scale on the *y*-axis for the two measurements) can be seen just after 11:25 in the emission zone, when the outflow filter is removed. The CPC (>0.007 µm) shows the most prominent increase, but the APS (>0.5 µm) also shows an increase at this time, even though it is lower. The instruments measuring in the personal breathing zone did not show any significant particle increases.

The filters sampled during exchange of NW outflow filter(s) (during Study 2) showed elevated concentrations of Ga (0.51 µg/m^3) and As (3.6 µg/m^3), see Table 3, confirming a probable emission of GaAs containing particles.

Sonication of substrates with Si nanowires

Fig. 7 shows the total particle number concentration in the post-production laboratory during Study 2, during sonication of 14 different substrates with Si nanowires. Short particle peaks can be seen for particles both in the

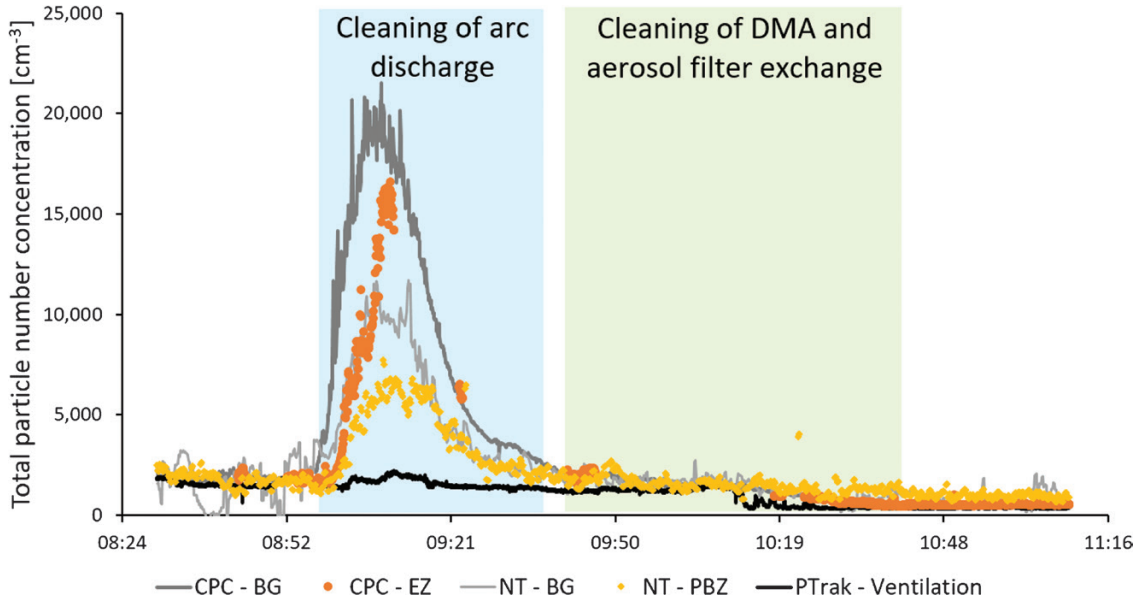

Figure 1. Cleaning of arc discharge and DMA and aerosol filter exchange in the production laboratory measured during Study 2. Total particle number concentration measured in the emission zone, EZ (with CPC, >0.007 µm), the personal breathing zone, PBZ (with Nanotracer (NT), 0.01–0.3 µm), the background zone, BG (with CPC and Nanotracer), and the ventilation supply air (with P-Trak, 0.02–1 µm).

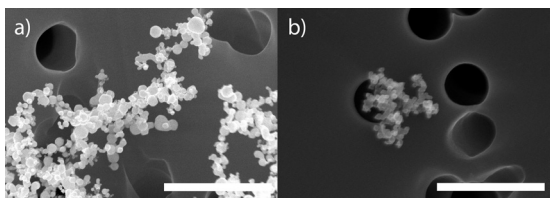

Figure 2. SEM images of gold particles (confirmed with EDX) found in (a) the emission zone and (b) the personal breathing zone during Study 2, during cleaning of arc discharge and DMA and aerosol filter exchange in the production laboratory. The bar equals 1 µm.

nanometer range and the micrometer range in the emission zone during the repetitive work of handling the substrates. The sonication procedure was preceded by one substrate being put in a bowl, which was covered with Para film and then placed in the sonication bath. The specific activity that generated the peaks seen in Fig. 7 is the removal of the Para film after sonication. The instruments measuring in the personal breathing zone did not show any significant particle increases. Fig. 8 shows the aerodynamic particle size distribution from the emission and the background zone during the presence of peak 12 in Fig. 7 (at ~12:14).

SEM and EDX analysis of the filter sampled during sonication of substrates with Si nanowires (Study 2), in the emission zone, confirmed the presence of Si nanowires (Fig. 9).

The remaining work tasks (inspection of reactor, automatic reactor cleaning, leak test, work in glove box, production of GaAs NWs, and handling of substrates with Si NWs) did not generate any significant particle emissions above background, neither in the emission zone nor in the personal breathing zone, indicating that there is a minimal potential for exposure during these specific processes.

Sampling of arsine gas

During Study 1, no arsine could be detected in any of the samples, therefore, during Study 2, no arsine sampling was conducted.

Surface sampling

Of the 32 workplace surfaces sampled in the production and post-production laboratories during Study 1, only one surface, the striated metal floor inside the reactor enclosure, was contaminated with nanowires (Fig. 10a). Of the 18 sampled workplace surfaces in the production and post-production laboratories during Study 2, nanowires were found only on one surface, again the floor inside the reactor enclosure (Fig. 10b). Quantitation was not possible due to overload on the tape samples.

Discussion

To our knowledge, this is the first study characterizing exposure and emissions of aerotaxy produced

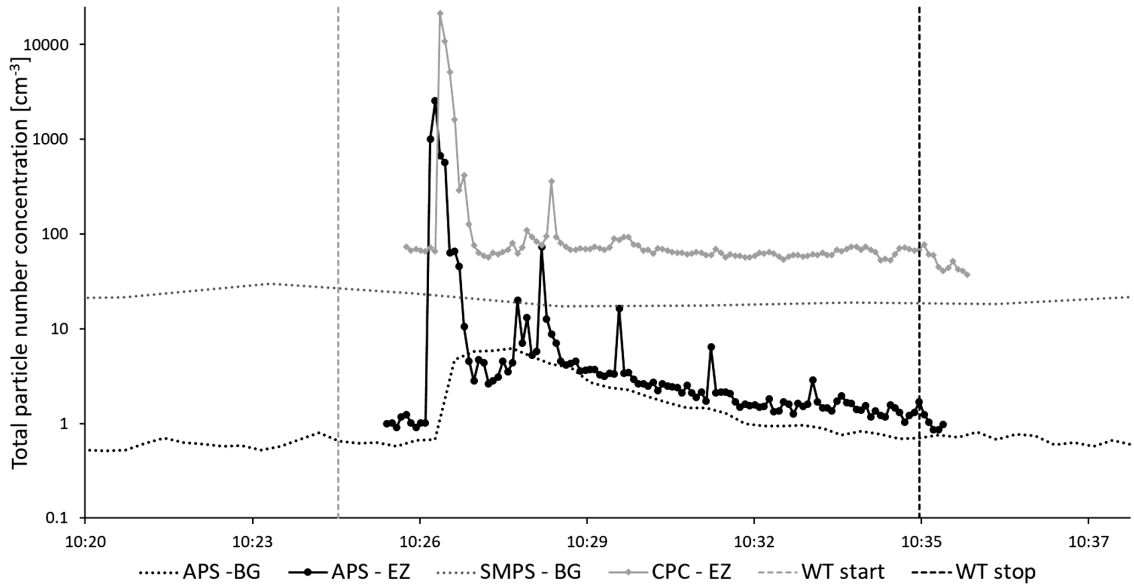

Figure 3. Manual reactor cleaning in the production laboratory measured during Study 1. Total particle number concentration measured in the emission zone, EZ (with APS, 0.5–20 μm, and CPC, >0.007 μm) and the background zone, BG (with APS and SMPS, 0.01–0.5 μm).

semiconductor nanowires. Our results indicate that a major part of the potential exposure occurs not during the actual manufacturing, but during the cleaning and maintenance procedures. This has also previously been shown at other nanoparticle facilities (Nilsson et al., 2013; Hedmer et al., 2014; Fonseca et al., 2015; Kaminski et al., 2015; Ludvigsson et al., 2016). In Study 2, cleaning of the arc discharge and the DMA, which is used for generation and size selection of the seed particles, generated emissions that were not only obvious in the emission zone instruments but also in the background (Fig. 1). When the work task began, the cleaning took place on a bench in the room with no extra ventilation. Since the P-Trak measurements in the supply air to the laboratory were relatively stable throughout the work task (as can be seen in Fig. 1), the particle emissions can be assumed to come from the cleaning activity alone. No other particle generating events took place elsewhere in the room, which points toward that the emissions from the cleaning procedure spread in the whole laboratory and thereby constitute a potential exposure for anyone present in the room. These measurements also corresponds well with the EDX detected gold on the filter samples (Fig. 2) collected during this work task, both from the emission zone and the personal breathing zone. Between 09:57 and 10:08 the cleaning of the outer part of the DMA took place inside an LAF-bench and between 10:36 and 10:41 one filter was exchanged. No particle increases could be seen for these activities. Based on these results, recommendations of conducting cleaning of the arc discharge in a fume hood have been forwarded to the producer. As can be seen in Fig. 1, the background CPC levels were higher than the emission zone CPC levels, and the same is true for the Nanotracer background levels when compared with the personal breathing zone Nanotracer levels. The CPCs and the Nanotracers were during part of the measurement day run as a side-by-side comparison, showing no significant discrepancy. It is not unlikely that some agglomeration can have occurred in the emission zone, which would locally have lowered the number concentration.

The direct-reading instruments (Fig. 3) showed high emissions during manual cleaning of the reactor (Study 1). Particle concentrations were several orders of magnitude larger than during any other work task. This peak was followed by several smaller emissions. During and after the first peak, an elevation in the background concentration was detected by the APS. It was not a large peak compared with the emission zone, but substantially higher than the rest of the background measurements. This work task, just as the cleaning of the arc discharge and the DMA, generates a potential risk of exposure for anyone present in the laboratory during this time. Manual reactor cleaning was also the only occasion during Study 1 where the Nanotracer, worn in the

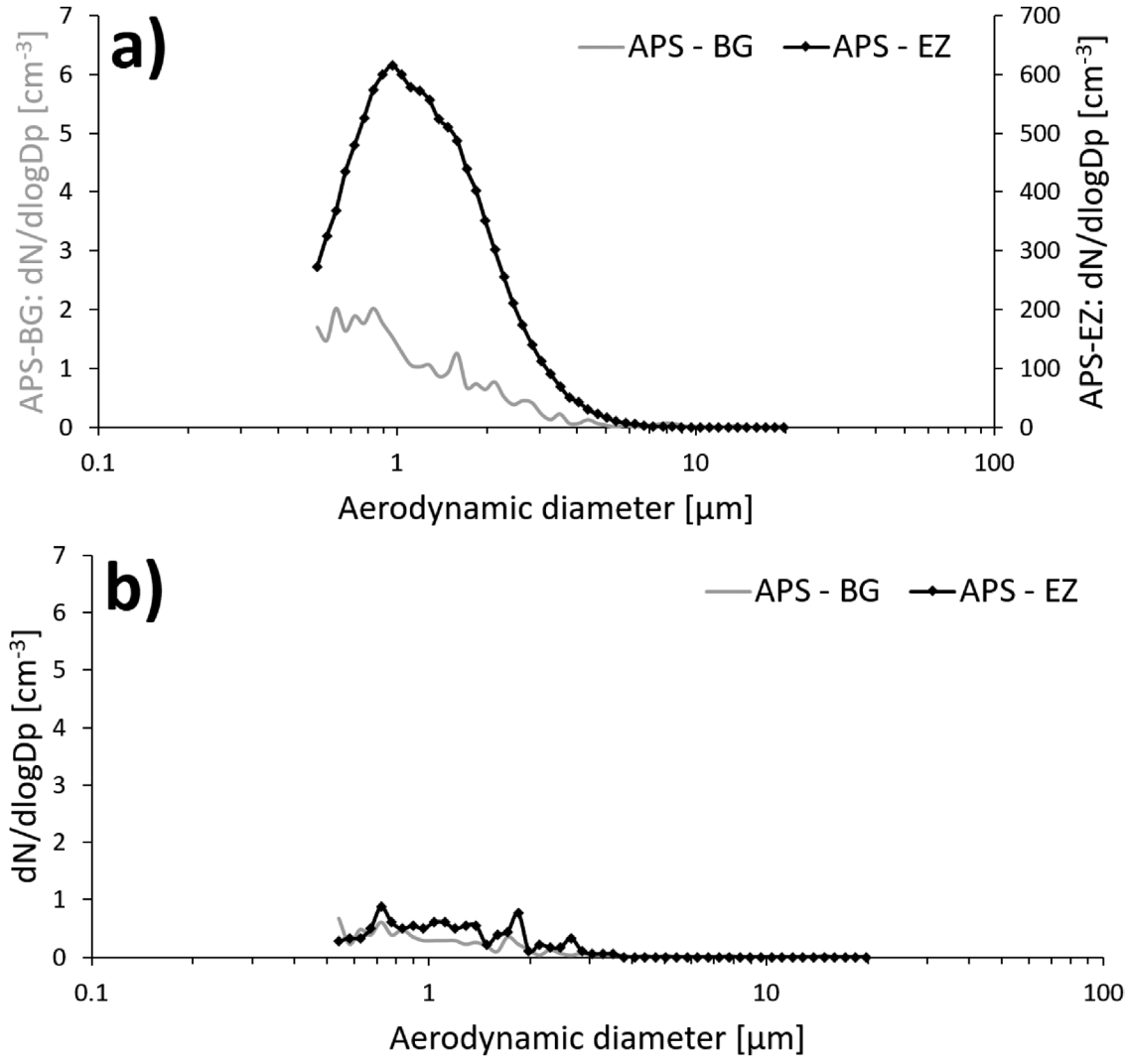

Figure 4. Aerodynamic particle size distribution measured in the emission zone (APS–EZ) and the background zone (APS–BG) during (a) the presence of the initial peak in Fig. 3 and (b) at the end of the work task shown in Fig. 3. Note the different scales in (a).

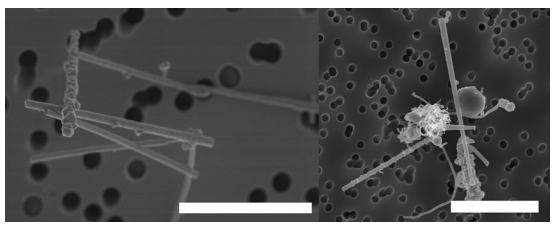

Figure 5. SEM images of parasitically grown GaAs nanowires found in (a) the emission zone, during manual reactor cleaning and in (b) the personal breathing zone during all the work tasks performed in the production laboratory. Sampling took place during Study 1. The bar in (a) equals 3 µm and the bar in (b) equals 5 µm.

personal breathing zone of the worker, showed particle concentrations large enough to be distinguished from the background noise level. The emissions generated during this work task are most likely the main reason for the Ga and As found in the background zone filters with ICP-MS. These emissions are also responsible for the fact that the particle concentration in the background in the production laboratory (Table 3) during Study 1 was an order of magnitude higher than during Study 2, see Fig. 3. Also, nanowires were present on the floor of the reactor during both Studies 1 and 2 (Fig. 10a,b). Important findings are also that manual reactor cleaning generated nanowire number concentrations of 98 cm^{-3}

Table 4. Characteristics of the sampled nanowires in Study 1. The statistics are based on 100 nanowires evaluated by SEM.

	Length (µm)	Width (µm)	Aspect ratio (L/W)
Mean (µm)	3.88	0.36	14.29
Median (µm)	3.25	0.29	9.52
Range	0.52 < L < 24.76	0.075 < W < 1.95	2.72 < AR < 77.05

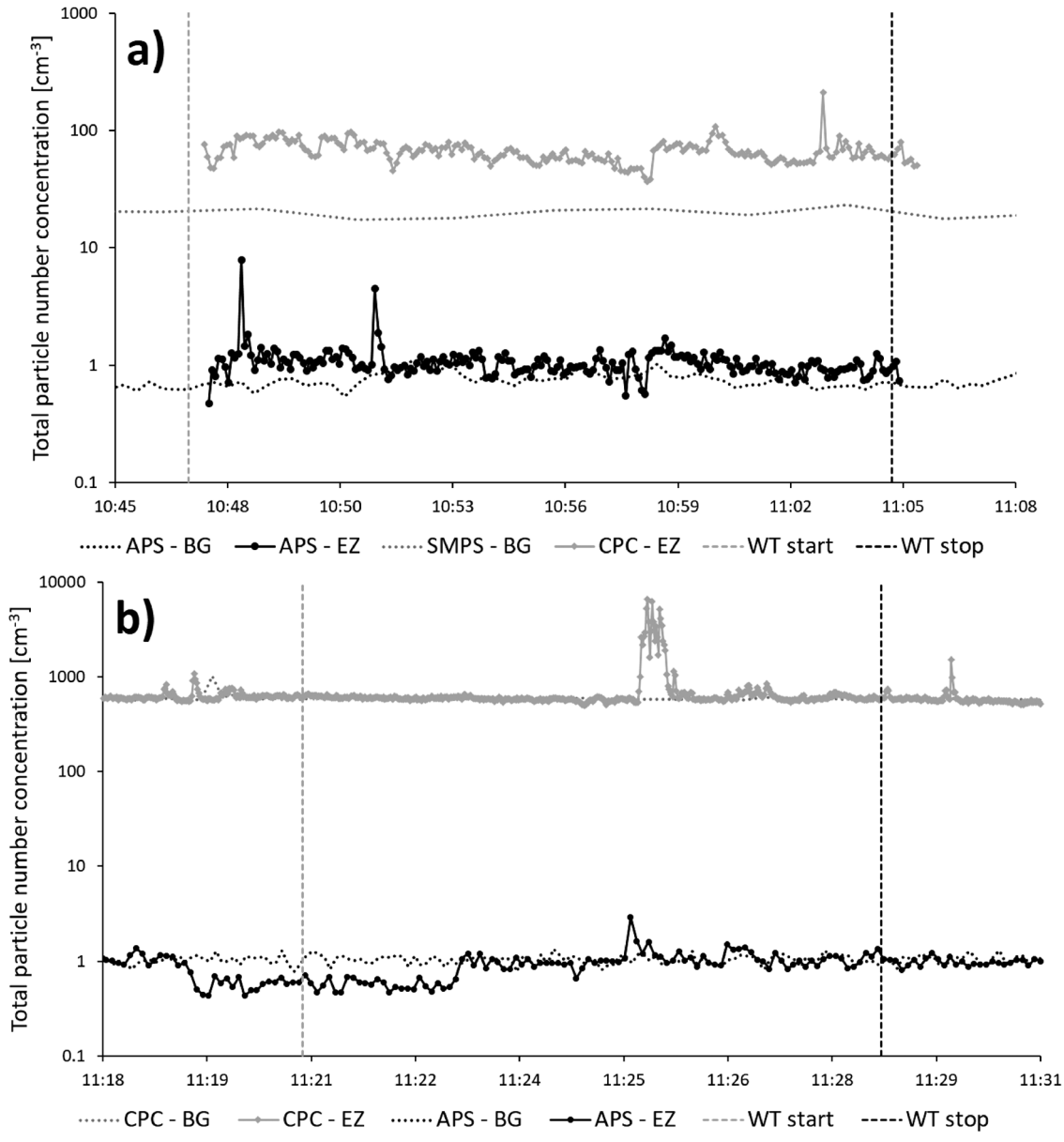

Figure 6. Exchange of NW outflow filter(s) in the production laboratory during (a) Study 1 and (b) Study 2. Total particle number concentration measured in the emission zone, EZ (with APS, 0.5–20 µm, and CPC, >0.007 µm) and the background zone, BG (with APS and SMPS, 0.01–0.7 µm/CPC). Note the difference on the scale of the *y*-axis.

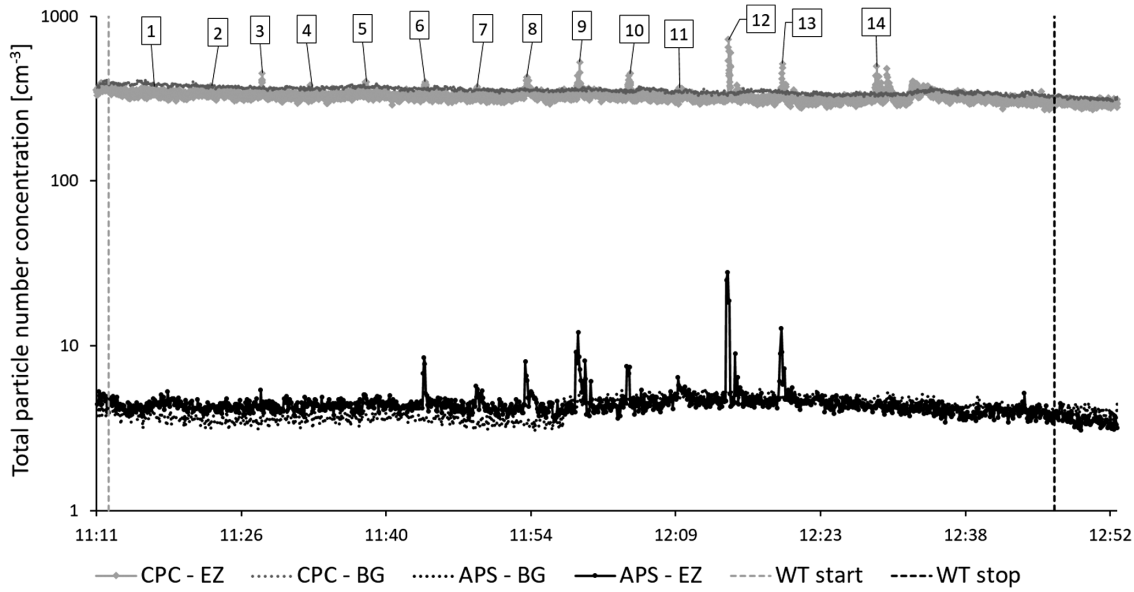

Figure 7. Sonication of substrates with Si nanowires in the post-production laboratory measured during Study 2. Total particle number concentration measured in the emission zone, EZ (with APS, 0.5–20 µm, and CPC, >0.007 µm) and the background zone, BG (with APS and CPC). The numbers indicate when the 14 different substrates were handled during the work task.

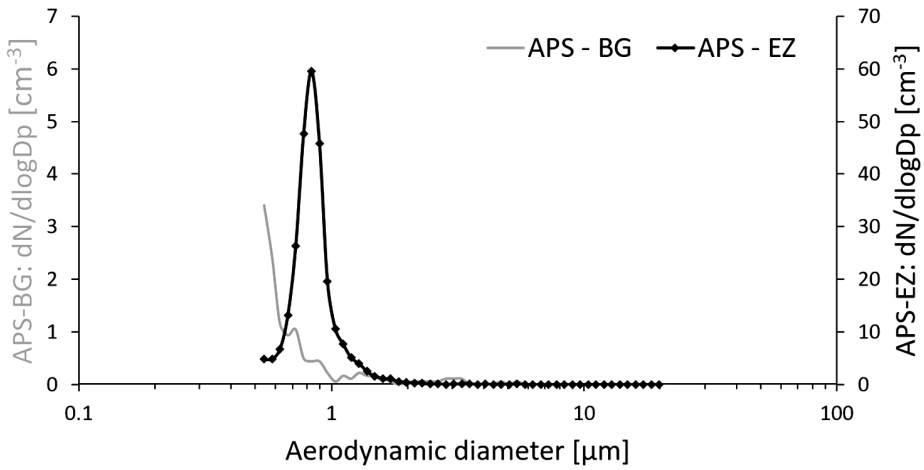

Figure 8. Aerodynamic particle size distribution measured in the emission zone (APS–EZ) and the background zone (APS–BG) during the presence of peak 12 in Fig. 7. Note the different scales.

in the emission zone and 0.025 cm^{-3} in the personal breathing zone, corresponding to an 8-h time weighed average (8-h TWA) of 0.013 cm^{-3}. Currently, there are no standard nanofiber collection techniques designed for workplace settings (Koivisto et al., 2018) and also, there is according to NIOSH, an inter laboratory variability in a fiber counting method (since the results of the method is based on randomly selected areas of the filter), which can add a significant uncertainty to the obtained concentrations in the emission- and personal breathing zone (US National Institute for Occupational Safety and Health (NIOSH), 2016). Assuming that all the studied nanowires are nanowires according to the WHO criteria and have similar toxicity as Mitsui carbon nanotubes (Bornholdt et al., 2017), they should obey under the same suggested occupational exposure limit value for fibrous nanomaterials of 0.01 cm^{-3} as an 8-h TWA (British Standards (BSI), 2007; Van Broekhuizen

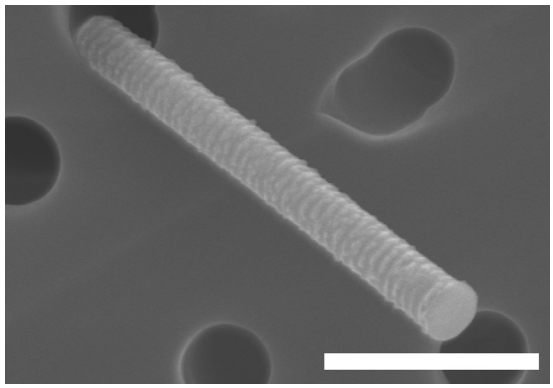

Figure 9. SEM image of a Si nanowire (confirmed with EDX) found in the emission zone during sonication of substrates with Si nanowires (Study 2). The bar equals 1 µm.

et al., 2012; German Hazardous Substances Committee, 2013; Stockmann-Juvala, 2014). Thus, a measured TWA of 0.013 cm^{-3} can pose a health risk. It is also worth noticing that suggested nanofiber OELs assume that the exposure is measured as primary nanofibers. Workplace studies have, however, shown that most emitted nanofibers—as well as nanoparticles in general—are present mainly in agglomerated forms (Hedmer et al., 2014; Mihalache et al., 2017), and there is still no consensus on how to take this into account. It has also been pointed out that the scientific methods used for deriving OELs, and their associated outcomes, differ widely (Harrison et al., 2015). The wide aerodynamic size distribution (seen in Fig. 4a) found during the high emission peak during manual reactor cleaning, confirm that the nanofiber emissions do occur as larger agglomerates, in the micrometer range. When no emissions are present, the two APSes measures very similar, as can be seen in Fig. 4b, which also corresponds well with the side-by-side comparison conducted during part of the measurement day (where no significant discrepancies were seen). Additionally, in the count of fibers matching the WHO criteria, it should be taken into account that SEM images (such as Fig. 5a) show fibers that do not lie flat on the filter surface. Based on the 2D-projection of a 3D object, length measurements can be underestimations, also leading to an underestimation of the count of fibers matching the WHO criteria.

An important finding in this study was that the emitted nanowires were much longer (up to almost 25 µm) than the primary produced nanowires (which were ~1 µm) (Table 4 and Fig. 5). This is of importance for health risk assessments of the work procedure and the occupationally exposed worker, since deposition of insoluble fibers longer than 5 µm will result in

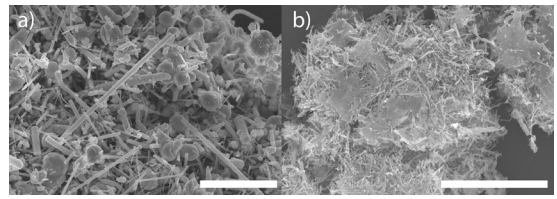

Figure 10. SEM images of parasitically grown nanowires found on the floor inside the reactor enclosure in the production laboratory during the measurements in (a) Study 1 and (b) Study 2. The bar equals 10 µm.

frustrated phagocytosis which, in turn, could cause inflammation, granuloma formation, and fibrosis in the lungs (Donaldson et al., 2010). These results were communicated to the producer and, after upscaling of the nanowire production, the manual cleaning of the reactor was abolished.

Exchange of nanowire outflow filters in the production laboratory was conducted somewhat differently during Study 1 and Study 2 due to a different apparatus setup after the upscaling. Three filters were changed during Study 1, generating only minor emissions (Fig. 6a). After upscaling (Study 2), only one filter needed to be changed (an upscaling engineering control to reduce the potential exposure of having to change several filters). This work task, unlike when being conducted during Study 1, produced a measurable concentration increase in the emission zone (Fig. 6b), which likely is a result of the larger amount of material that is being handled due to the upscaling. No corresponding increase could be detected in the background zone, which indicates that this work task does not generate an exposure risk for anyone else but the person who changes the filter. During Study 1, the work was conducted in a clean room, which was not the case during Study 2, which explains the higher background levels measured in Study 2. The fact that no nanomaterial could be detected by SEM during this work task in Study 2 (see Table 3) is due to the short sampling time.

Another result of the upscaling, which poses a potential increased risk of exposure, is the short particle peaks in the emission zone during sonication (Fig. 7). During this work task in Study 2, 14 different substrates with Si nanowires were handled consecutively. They were placed in a bowl with ethanol, the bowl was covered with Para film, placed in the sonication bath and sonicated for about 2–3 min. The bowl was then lifted out of the sonication bath, the Para film was removed and disposed of in a collection bin, and the substrate was removed, rinsed off, and put on a paper at the side. Almost all of these cycles were visible in the CPC (which measures

particles >0.007 µm) and APS (which measures particles 0.5–20 µm) with the peaks being the result of the Para film being removed from the bowl after sonication. The narrow aerodynamic size distribution (Fig. 8), found when the Para film was being removed, indicates that these emissions are of another kind compared with the emissions found during manual reactor cleaning (wide size distribution). Cleaning procedures seem to cause emissions of different sized agglomerates while the Para film removal more extensively generates emissions of the single nanowires. These measurements also correspond well with the detected Si nanowires on the filter samples (Fig. 9) collected in the emission zone during this work task. The upscaling, in this case, means that more substrates than before are being handled during sonication, which increases the overall emissions and hence the potential exposure. The level of these emissions may differ depending on the individual worker who performs the task. Thus, this production step should be performed with exposure control techniques, e.g. inside a fume hood.

In Studies 1 and 2, GaAs nanowire surface contamination was detected only inside the reactor enclosure, indicating that the surface contamination was limited. Thus, the concern and risk of secondary inhalation exposure and dermal exposure seem to be limited to the worker who opens up the reactor enclosure. Unfortunately, it was not possible to quantitate the tape samples collected from the surface inside the reactor enclosure due to overload of material. With the tape sampling method, it is possible to survey the presence of surface contamination of nanomaterial at workplaces (Hedmer et al., 2015). A widely spread surface contamination increases the risk of dermal exposure but also secondary inhalation exposure through resuspension of contamination deposited on workplace surfaces.

There may be a slight uncertainty in the digestion method for the filter samples in ICP-MS due to the acid used. Possibly a combination of stronger acids may be required to dissolve all the collected GaAs containing particles (US National Institute for Occupational Safety and Health (NIOSH), 1994). Thus, it is possible that the determined metal concentrations of As and Ga are somewhat underestimated. However, the results from the metal composition analysis seem to be consistent with the results from the SEM analysis for example during manual reactor cleaning.

If inhaled, fiber-shaped particles are of health concern. Asbestos is a high-aspect-ratio particle which is well known to, due to the small diameter, penetrate the alveoli wall, be translocated to the pleura and cause mesothelioma, a characteristic type of pleural cancer. Carbon nanotubes have structural similarities to asbestos fibers and several studies show that they can induce similar adverse biological effects. Multi-walled carbon nanotubes used in animal inhalation models have resulted in serious lung effects such as inflammation, mesothelioma, granuloma formation, and fibrosis, even at relatively low doses (Ma-Hock et al., 2009; Ryman-Rasmussen et al., 2009; Pauluhn, 2010; Porter et al., 2013; Chernova et al., 2017). Carbon nanotubes have also shown to penetrate both alveolar macrophages, the alveolar wall and the visceral pleura (Mercer et al., 2010). At least two animal studies have shown carcinogenicity (Rittinghausen et al., 2014; Kasai et al., 2016), and Mitsui 7 carbon nanotubes have been classified by IARC (International Agency for Research on Cancer) as possibly carcinogenic to humans (group 2B) (International Agency for Research on Cancer (IARC), 2017). A study (Fatkhutdinova et al., 2016) of workers exposed to relatively high occupational levels of carbon nanotubes found a significant increase in fibrosis markers in collected sputum samples. For semiconductor nanowires, no conclusive results from inhalation studies are available (solubility data is missing), but given their similarity to carbon nanotubes in terms of size and shape it can be assumed that occupational inhalation exposure of nanowires could be harmful to health. It could also be assumed that there is no lower threshold concentration under which exposure is safe. This is especially valid if the nanowires are produced in aerosol phase, which would increase the risk of airborne exposure, and if they are bio persistent. Ions of arsenic are highly toxic to humans and gallium may have a significant toxicity and may cause cancer (US National Institute for Occupational Safety and Health (NIOSH), 1987; White and Shine, 2016). Probably, the toxicities of gallium arsenide are related primarily to the arsenic component of this compound, but other gallium compounds display antineoplastic and antimicrobial activities (Chitambar, 2010). Gallium arsenide, as a bulk material, is carcinogenic to humans (Group 1) (International Agency for Research on Cancer (IARC), 2006). In Sweden, there is an occupational exposure limit for arsenic and its inorganic compounds set to 0.01 mg/m^3 but no occupational exposure limits have been set for gallium (Swedish Work Environment Authority, 2018). However, the American Conference of Governmental Industrial Hygienists has recommended a threshold limit value for gallium arsenide to be 0.3 µg/m^3 (respirable fraction) (American Conference of Governmental Industrial Hygienists (ACGIH), 2019). Currently, there are knowledge gaps regarding the solubility of GaAs nanowires in the lung. However, previous studies of silver and nickel nanowires have shown to be

pathogenic in the pleura (Schinwald et al., 2012) and induce persistent inflammation and fibrosis in the pleural or peritoneal linings (Poland et al., 2012). Thus, if GaAs nanowires are insoluble in the lungs the stiff fiber shape poses potential for a similar risk in the lungs as by inhalation of asbestos and carbon nanotubes.

The toxicity of silicon nanowires is not so well studied yet. Roberts et al. (2012) tested the pulmonary toxicity in rats by intratracheally instillation of silicon nanowires and found that silicon nanowires induced transient lung toxicity but it may lead to increased collagen deposition in the lung due to dose or nanowire length. The silicon nanowires present during this study were only used as example nanowires for exposure evaluations and are not produced or used by the company. However, silicon nanowires can be manufactured for applications in, e.g. sensors and transistors for circuits.

Until the toxicity of semiconductor nanowires is fully known, the precautionary principle must reign at all times during production and handling of nanowires. In practice, this means closed handling of nanowires in combination with a high level of engineering controls and a high degree of PPE (i.e. powered air-purifying respirators with adequate gas and particulate filters) (Koivisto et al., 2015).

Conclusions

Exposures and emissions of aerotaxy-produced semiconductor nanowires were, for the first time, characterized through measurements during production, post-production, and maintenance at a metal nanowire producer. Our results show that the majority of the potential exposure occurs not during the actual manufacturing, but during the cleaning and maintenance procedures of, e.g. the aerotaxy reactor. The emitted nanowires were much longer than the primary produced, which is important knowledge for risk assessments. The exposures and emissions were evaluated pre- and post-upscaling the production and showed that some work tasks (e.g. exchange of nanowire outflow filters and sonication of substrates with nanowires) had an increase of emissions post-upscaling.

Acknowledgements

The project was funded by AFA insurance (Dnr 130122) and NanoLund (p38-2013), and was carried out within the framework of NanoLund at Lund University. The project sponsors have only contributed financially and have not participated in preparing the research material, writing, reviewing, or approving the submitted manuscript. The nanowire producer, where the measurements were performed, have read and approved the final version of the manuscript without any corrections.

Declaration

The authors declare no conflict of interest relating to the material presented in this article.

References

American Conference of Governmental Industrial Hygienists (ACGIH). (2019). *TLVs and BEIs*. Cincinnati, OH: ACGIH.

Barkauskas J, Stankeviciene I, Selskis A. (2010). A novel purification method of carbon nanotubes by high-temperature treatment with tetrachloromethane. *Separ Purific Technol*; **71**: 331–336.

Bornholdt J, Saber AT, Lilje B, *et al.* (2017). Identification of gene transcription start sites and enhancers responding to pulmonary carbon nanotube exposure in vivo. *ACS Nano*; **11**: 3597–3613.

British Standards (BSI). (2007). *Nanotechnologies – part 2: guide to safe handling and disposal of manufactured nanomaterials*. *PD* 6699-2:2007. London, UK: BSI.

Chan CK, Peng HL, Liu G, *et al.* (2008). High-performance lithium battery anodes using silicon nanowires. *Nat Nanotechnol*; **3**: 31–35.

Chernova T, Murphy FA, Galavotti S, *et al.* (2017). Long-fiber carbon nanotubes replicate asbestos-induced mesothelioma with disruption of the tumor suppressor gene Cdkn2a (Ink4a/Arf). *Curr Biol*; **27**: 3302.

Chitambar CR. (2010). Medical applications and toxicities of gallium compounds. *Int J Environ Res Public Health*; **7**: 2337–2361.

Contado C. (2015). Nanomaterials in consumer products: a challenging analytical problem. *Front Chem*; **3: 48**.

Donaldson K, Murphy FA, Duffin R. *et al.* (2010). Asbestos, carbon nanotubes and the pleural mesothelium: a review of the hypothesis regarding the role of long fibre retention in the parietal pleura, inflammation and mesothelioma. *Particle Fibre Toxicol*; **7: 5**.

European Commission. (2011). Commission recommendation of 18 October 2011 on the definition of nanomaterial (2011/696/EU). *Off J Eur Union*; **275**: 38–40.

Fatkhutdinova LM, Khaliullin TO, Vasil'yeva OL, *et al.* (2016). Fibrosis biomarkers in workers exposed to MWCNTs. *Toxicol Appl Pharmacol*; **299**: 125–131.

Fonseca AS, Viitanen AK, Koivisto AJ, *et al.* (2015). Characterization of exposure to carbon nanotubes in an industrial setting. *Ann Occupat Hyg*; **59**: 586–599.

German Hazardous Substances Committee, A. B. (2013). *Announcement on hazardous substances 527 (BekGS 527) BAuA*. Dortmund, Germany: BAuA.

Harrison P, Holmes P, Bevan R, *et al.* (2015). Regulatory risk assessment approaches for synthetic mineral fibres. *Regul Toxicol Pharmacol*; **73**: 425–441.

Hedmer M, Isaxon C, Nilsson PT, *et al.* (2014). Exposure and emission measurements during production, purification, and functionalization of arc-discharge-produced multi-walled carbon nanotubes. *Ann Occupat Hyg*; **58**: 355–379.

Hedmer M, Ludvigsson L, Isaxon C, *et al.* (2015). Detection of multi-walled carbon nanotubes and carbon nanodiscs on workplace surfaces at a small-scale producer. *Ann Occupat Hyg*; **59**: 836–852.

Heurlin M, Magnusson MH, Lindgren D, *et al.* (2012). Continuous gas-phase synthesis of nanowires with tunable properties. *Nature*; **492**: 90.

International Agency for Research on Cancer (IARC). (2006). IARC Monographs on the evaluation of carcinogenic risks to humans. *Cobalt in hard metals and cobalt sulfate, gallium arsenide, indium phosphide and vanadium pentoxide*. **86**.

International Agency for Research on Cancer (IARC). (2017). IARC monographs on the evaluation of carcinogenic risks to humans. *Some Nanomaterials and Some Fibres*; **111**.

Kaminski H, Beyer M, Fissan H, *et al.* (2015). Measurements of nanoscale TiO2 and Al2O3 in industrial workplace environments - methodology and results. *Aerosol Air Qual Res*; **15**: 129–141.

Kane AB, Hurt RH, Gao HJ. (2018). The asbestos-carbon nanotube analogy: an update. *Toxicol Appl Pharmacol*; **361**: 68–80.

Kasai T, Umeda Y, Ohnishi M, *et al.* (2016). Lung carcinogenicity of inhaled multi-walled carbon nanotube in rats. *Particle Fibre Toxicol*; **13**: 53.

Koivisto AJ, Aromaa M, Koponen IK, *et al.* (2015). Workplace performance of a loose-fitting powered air purifying respirator during nanoparticle synthesis. *J. Nanoparticle Res*., **17**: 177.

Koivisto AJ, Bluhme AB, Kling KI, *et al.* (2018). Occupational exposure during handling and loading of halloysite nanotubes – a case study of counting nanofibers. *Nanoimpact*; **10**: 153–160.

Ludvigsson L, Isaxon C, Nilsson PT, *et al.* (2016). Carbon nanotube emissions from arc discharge production: classification of particle types with electron microscopy and comparison with direct reading techniques. *Ann Occupat Hyg*; **60**: 493–512.

Ma-Hock L, Treumann S, Strauss V, *et al.* (2009). Inhalation toxicity of multiwall carbon nanotubes in rats exposed for 3 months. *Toxicol Sci*; **112**: 468–481.

Mcintyre RA. (2012). Common nano-materials and their use in real world applications. *Sci Prog*; **95**: 1–22.

Mercer RR, Hubbs AF, Scabilloni JF, *et al.* (2010). Distribution and persistence of pleural penetrations by multi-walled carbon nanotubes. *Particle Fibre Toxicol*; **7**: 28.

Messing ME, Hillerich K, Johansson J, *et al.* (2009). The use of gold for fabrication of nanowire structures. *Gold Bulletin*; **42**: 172–181.

Mihalache R, Verbeek J, Graczyk H, *et al.* (2017). Occupational exposure limits for manufactured nanomaterials, a systematic review. *Nanotoxicology*; **11**: 7–19.

Nilsson PT, Isaxon C, Eriksson AC, *et al.* (2013). Nano-objects emitted during maintenance of common particle generators: direct chemical characterization with aerosol mass spectrometry and implications for risk assessments. *J Nanoparticle Res*; **15**: 2052.

Pauluhn J. (2010). Subchronic 13-week inhalation exposure of rats to multiwalled carbon nanotubes: toxic effects are determined by density of agglomerate structures, not fibrillar structures. *Toxicol Sci*; **113**: 226–242.

Poland CA. (2011). *Toxicology of high aspect ratio nanomaterials based on the fibre pathogenicity paradigm structure-activity relationship of pathogentic fibres*. Doctoral thesis, Scotland, UK: University of Edinburgh.

Poland CA, Byrne F, Cho WS, *et al.* (2012). Length-dependent pathogenic effects of nickel nanowires in the lungs and the peritoneal cavity. *Nanotoxicology*; **6**: 899–911.

Porter DW, Hubbs AF, Chen BT, *et al.* (2013). Acute pulmonary dose-responses to inhaled multi-walled carbon nanotubes. *Nanotoxicology*; **7**: 1179–1194.

Qian F, Gradecak S, Li Y, *et al.* (2005). Core/multishell nanowire heterostructures as multicolor, high-efficiency light-emitting diodes. *Nano Letters*; **5**: 2287–2291.

Rittinghausen S, Hackbarth A, Creutzenberg O, *et al.* (2014). The carcinogenic effect of various multi-walled carbon nanotubes (MWCNTs) after intraperitoneal injection in rats. *Particle Fibre Toxicol*; **11**: 59.

Roberts JR, Mercer RR, Chapman RS, *et al.* (2012). Pulmonary toxicity, distribution, and clearance of intratracheally instilled silicon nanowires in rats. *J Nanomater*; **2012**: 398302.

Ryman-Rasmussen JP, Tewksbury EW, Moss OR, *et al.* (2009). Inhaled multiwalled carbon nanotubes potentiate airway fibrosis in murine allergic asthma. *Am J Resp Cell Mol Biol*; **40**: 349–358.

Schinwald A, Murphy FA, Prina-Mello A, *et al.* (2012). The threshold length for fiber-induced acute pleural inflammation: shedding light on the early events in asbestos-induced Mesothelioma. *Toxicol Sci*; **128**: 461–470.

Stockmann-Juvala H, Taxell P, Santonen T. (2014). *Formulating occupational exposure limit values (OELs) (Inhalation & Dermal)*. Helsinki: Finnish Institute of Occupational Health.

Swedish Work Environment Authority. (2018). *AFS 2018:1, Occupational exposure limits [Hygieniska gränvärden]*. Stockholm, Sweden: Anna Varg.

Tanaka A. (2004). Toxicity of indium arsenide, gallium arsenide, and aluminium gallium arsenide. *Toxicol Appl Pharmacol*; **198**: 405–411.

US National Institute for Occupational Safety and Health (NIOSH). (1987). *Reducing the potential risk of developing cancer from exposure to gallium arsenide in the microelectronics industry*. Cincinnati, OH: NIOSH.

US National Institute for Occupational Safety and Health (NIOSH). (1994). *Manual of analytical methods (NMAM)*. 4th edn, ARSENIC and compounds, as As. 7900. Cincinnati, OH: NIOSH.

US National Institute for Occupational Safety and Health (NIOSH). (2016). *Manual of analytical methods (NMAM)*. 5th edn. Cincinnati, OH: NIOSH.

Van Broekhuizen P, Van Veelen W, Streekstra WH, *et al.* (2012). Exposure limits for nanoparticles: report of an international workshop on nano reference values. *Ann Occupat Hyg*; **56**: 515–524.

Wallentin J, Anttu N, Asoli D, *et al.* (2013). InP nanowire array solar cells achieving 13.8% efficiency by exceeding the ray optics limit. *Science*; **339**: 1057–1060.

White SJ, Shine JP. (2016). Exposure potential and health impacts of indium and gallium, metals critical to emerging electronics and energy technologies. *Curr Environ Health Rep*; **3**: 459–467.

WHO. (1986). *Asbestos and other natural mineral fibres. Environmental health criteria*. Geneva: World Health Organization.

WHO. (1997). *Determination of airborne fibre number concentrations: a recommended method, by phasecontrast optical microscopy (membrane filter method)*. Geneva: World Health Organization.

Yazawa M, Koguchi M, Muto A, *et al.* (1992). Effect of one monolayer of surface gold atoms on the epitaxial-growth of InAs nanowhiskers. *Appl Phys Lett*; **61**: 2051–2053.